Modeling of the Catalytic Distillation Process for the Synthesis of Dimethyl Carbonate by Urea Methanolysis Method

Feng Wang,[†,‡] Ning Zhao,[†] Junping Li,[†] Wenbo Zhao,[†,‡] Fukui Xiao,[†] Wei Wei,[†] and Yuhan Sun*[,†]

State Key Laboratory of Coal Conversion, Institute of Coal Chemistry, Chinese Academy of Sciences, Taiyuan, 030001, P R China, and Graduate School of the Chinese Academy of Sciences, Beijing, 100039, China

A nonequilibrium model of the catalytic distillation was developed for the process of DMC synthesis by a urea methanolysis method over a solid base catalyst at the bench scale, and the Wilson model was used to account for the nonideality of the liquid phase. The superiority of the catalytic distillation on the removal of the products to restrain the reverse reaction was illustrated in the present work. Furthermore, the influence of total pressure and the reaction temperature on DMC yield and the sensitivity analysis to the reaction kinetics were discussed in detail. The results revealed that the catalytic distillation was appropriate for the process of DMC synthesis.

Introduction

Much attention has been paid to the synthesis of dimethyl carbonate (DMC), which is considered as an environmentally benign building block and is widely used in chemical industry. DMC can be used as a methylation reagent to substitute extremely toxic dimethyl sulfate or methyl halides and as a carbonylation reagent for replacing phosgene.[1−4] It has been conventionally produced from phosgene and methanol, and this route is limited in industry for usage of the extra toxic materials. The current routes for DMC synthesis are the oxycarbonylation of methanol (EniChem process and UBE process) and the transesterification method (Texaco process),[5] but these routes suffer from the use of poisonous or corrosive gases of chlorine, nitrogen oxides, and carbomonoxide and bearing the possibility of explosion.[6−9] The route of DMC synthesis by the transesterification method is limited by the thermodynamic equilibrium conversion, which leads to a low production of DMC. Recently, an attractive route for the synthesis of DMC by a urea methanolysis method over solid base catalyst has been carried out in a catalytic distillation.[10]

The catalytic distillation (CD), which is also known as reactive distillation that combines the heterogeneous catalyzed chemical reaction and distillation in a single unit, has attracted more interest in academia and become more important in the chemical processing industry as it has been successfully used in several important industrial processes.[11] The CD provides some advantages such as high conversion in excess of the chemical equilibrium, energy saving, overcoming of the azeotropic limitations, and prolonging the catalyst lifetime.[12−15] The number of contributions for both the simulative and experimental investigations about catalytic distillation are greatly increasing in recent years, especially for the modeling and simulation studies, and the applications of the catalytic distillation in its field is expending.[16] The modeling analysis approach for the design, synthesis, and feasibility analysis of the reactive distillation process has been parallely developed since the equilibrium stage model had been used for process analysis through computer in late 1950s.[17] However, a real distillation process always operates away from equilibrium, and for multicomponent mass transfer in the distillation, the stage efficiency is often different for each component.[18] In recent years, the nonequilibrium model, also called rate-based model, has been developed for a reactive distillation column to describe the mass transfer between vapor and liquid phase using the Maxwell−Stefan equations.[19−21] A detailed nonequilibrium model including the mass-transfer resistance betwen the liquid and porous catalyst for the methyl *tert*-butyl ether (MTBE) process has been given by Sundmacher and Hoffmann.[22] Lee and Dudukovic[23] have compared the nonequilibrium model with the equilibrium model for reactive distillation columns and obtained the information that the reaction rate was the main factor to affect the column behavior. A general review of the modeling approach using both equilibrium and nonequilibrium (rate-based) models of reactive distillation has been provided by Taylor and Krishna.[24]

In the presented work, the heterogeneously catalyzed reaction in the liquid bulk phase is considered as pseudohomogeneous for the synthesis of DMC. It should be noted that more complex three-phase models are developed in some contributions in recent years to rigorously describe the reaction kinetics and mass-transfer rate between the liquid and the solid catalytic phase in the catalyitc distillation. For example, Higler et al.[25] have incorporated the external mass-transfer resistence into the model and used the dusty fluid model to take into account mass transport inside the catalyst. Zheng et al.[26] and Hoffmann have treated the mass transfer of liquid with the catalyst as a third film between the liquid and solid phase. However, the authors also have claimed that a pseudohomogeneous nonequilibrium model might adequately simulate the temperature profile, yield, and selectivity for a CD process for a kineticlly controlled reaction system. Additionally, difficulties are related to the determination of additional model parameters required when using such models, and good estimation methods for the calculation of the diffusion coefficients and the nonideal thermodynamic behavior inside a catalyst are also absent.

However, most of the contributions focused on the synthesis processes of methyl acetate[12,27] or ethyl acetate[11] or the production of MTBE and *tert*-amyl methyl ether.[20,28−30] Podrebarac et al. investigated the production of diacetone alcohol with CD using a steady-state rate-based model.[19] Luo modeled the carbonylation process of ethanol with DMC, producing diethyl carbonate.[31] Zheng and Xu reported a CD process for the production of ethyl cellosolve and diacetone alcohol using

* To whom correspondence should be addressed. E-mail: yhsun@sxicc.ac.cn. Tel: +86+351+4049612,.Fax: +86+351+4041153.

[†] State Key Laboratory of Coal Conversion.

[‡] Graduate School of the Chinese Academy of Sciences.

10.1021/ie061480r CCC: $37.00
Published on Web 11/23/2007

Scheme 1. Synthesis of DMC from Urea and Methanol

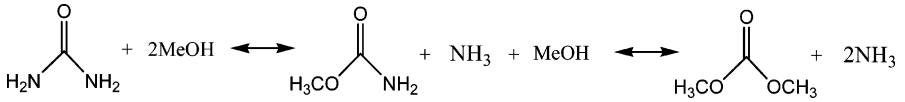

Table 1. Arrhenius Parameters for DMC Synthesis Catalyzed by Solid Base Catalyst

k_1 ($g^{-1}mol^{-1}L\ s^{-1}$)	k_2 ($g^{-1}mol^{-1}L\ s^{-1}$)	Ea_1 (J/mol)	Ea_2 (J/mol)
1.10×10^3	1.464×10^{-3}	1.01×10^5	4.90×10^4

the nonequilibrium model. But there was no report for the synthesis of DMC from urea and methanol by the CD process that was developed recently. In this work, modeling and simulation of such a catalytic distillation process for DMC synthesis from urea and methanol was carried out based on the nonequilibrium model, and the effect of distillation total pressure and the reaction temperature was studied; the interaction between the chemical reaction and the product separation were illustrated with the nonequilibrium model.

Chemical Reactions

The synthesis of DMC from urea and methanol is catalyzed by the solid base catalysts shown in Scheme 1.

The synthesis of DMC is a two-step reaction.[10,32] The intermediate methyl carbamate (MC) is produced with high yield in the first step and further converted to DMC by reacting with methanol on catalyst in the second step. Our co-workers have developed the ZnO catalyst to catalyze the DMC synthesis reaction in the CD process, which exhibited high activity toward the reactions.

It was found by our workers that the reaction of the first step took place with high yield even in the absence of catalyst, and the catalyst was mainly effective for the second step.[10] In the CD process for the synthesis of DMC, the material mixture of urea and methanol was fed in the CD column through a preheater, which has been heated to 423 K and the materials stayed in the preheater for sufficient time to convert the urea to MC. As a result, only the second step of the DMC synthesis reaction, where MC is converting to DMC, took place in the catalytic distillation column (shown as follows).

$$\mathrm{MC} + \mathrm{MeOH} \leftrightarrow \mathrm{DMC} + \mathrm{NH_3} \tag{1}$$

The macrokinetic model for the forward and reverse reactions by Arrhenius equations are represented as follows:

$$R = \omega k_1 \exp\left(-\frac{E_{a1}}{R_g T}\right) C_{MC} C_{Me} - \omega k_2 \exp\left(-\frac{E_{a2}}{R_g T}\right) C_{DMC} C_{NH_3} \tag{2}$$

where ω represents the amount of catalyst presented in the column section. k_1 and k_2 represent the Arrhenius frequency factors, and E_{a1} and E_{a2} are activation energy for the forward and reverse reactions, respectively. The values of the Arrhenius parameters for the synthesis of DMC by urea and methanol over the solid base catalyst are listed in Table 1.

The system of DMC synthesis process in a CD column mainly involved four components, methanol, DMC, MC, and ammonia, as the first step reaction was omitted in the distillation column (see Figure 1). The boiling points of the pure components at atmospheric pressure were ranged as follows: methanol (Me) 337.66 K; DMC 363.45 K; MC 450.2 K; ammonia (NH_3) 239.72 K. It could be seen that MC should almost exist in the liquid phase in the CD process under high pressure and the reactions would take place in the liquid phase in a CD reaction zone. The system included a binary azeotrope of Me−DMC and the predicted data are shown in Table 2, with respective boiling points at different pressures. Since the system included a no-condenser component of ammonia and a binary azeotropic pair of methanol−DMC, it shows the strong nonideal properties and the vapor liquid equilibrium were calculated by the EOS + activity method.

Nonequilibrium Model

The nonequilibrium model is schematically shown in Figure 2. This NEQ stage represents a section of packing in a packed column. The heterogeneously catalyzed synthesis of DMC in the CD process is treated as pseudohomogeneous. Mass transfers at the vapor−liquid interface are usually described via the well-known two-film model.[18] A rigorous model for catalytic distillation processes have been presented by Hegler, Taylor and Krishna.[20] In the present contribution, the two-phase nonequilibrium model have been developed to investigate the steady state of the DMC synthesis process in catalytic distillation.

The follow assumptions have been made for the nonequilibrium model: (1) the process reached steady state; (2) the first reaction has been omitted as it took place with high yield in the preheater; (3) the reactions occurred entirely in the liquid bulk; (4) the reactions have been considered as pseudohomogeneous; (5) the pressure in the CD column has been treated as constant.

The nonequilibrium model equations are described as below. The material balances both for vapor and liquid phase are defined as

$$V_{j+1} y_{i,j+1} - (1 + S_j^V) V_j y_{i,j} + F_j^V z_{i,j}^V - N_{i,j}^V = 0 \tag{3}$$

$$L_{j-1} x_{i,j-1} - (1 + S_j^L) L_j x_{i,j} + F_j^L z_{i,j}^L + N_{i,j}^L + R_{i,j}^L = 0 \tag{4}$$

The multicomponent mass-transfer rates are described by the generalized Maxwell−Stefan equations. The mass-transfer equations for liquid phase are described as follows:

$$-\frac{x_i}{R_g T} \nabla_T \mu_i = \sum_{\substack{j=1 \\ j \neq 1}}^{c} \frac{x_j N_i^L - x_i N_j^L}{C_t^L k_{ij}^L a} \tag{5}$$

where μ_i represents the chemical potential and k_{ij}^L is the liquid mass-transfer coefficient. Only $c - 1$ of these equations are independent. The vapor-phase mass transfer has a similar relation to the liquid phase.

The energy balances for both vapor and liquid phase are defined as

$$V_{j+1} H_{j+1}^V - (1 + S_j^V) V_j H_j^V + F_j^V H_j^{VF} - e_j^V + Q_j^V = 0 \tag{6}$$

$$L_{j-1} H_{j-1}^L - (1 + S_j^L) L_j H_j^L + F_j^L H_j^{LF} + e_j^L + H_j^{LR} + Q_j^L = 0 \tag{7}$$

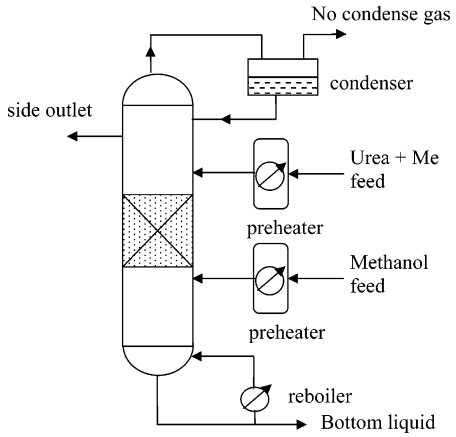

Figure 1. Scheme of the reactive distillation for DMC synthesis.

Table 2. Calculated Azeotropic Data of Me−DMC System

pressure (atm)	DMC (wt %)	T (°C)
1	29.7	65.2
2	25.8	82.8
4	20.6	104.2
8	14.5	129.6
12	10.0	145.6
15	7.0	153.9

where the vapor and liquid energy-transfer rate is considered as equal. The vapor heat-transfer rate is defined as

$$e^{\mathrm{V}} = -h^{\mathrm{V}} a \frac{\partial T^{\mathrm{V}}}{\partial \eta} + \sum_{i=1}^{C} N_i^{\mathrm{V}} H^{\mathrm{V}} \tag{8}$$

The vapor−liquid equilibrium occurs at the vapor−liquid interface:

$$y_{i,j}^{\mathrm{I}} - K_{i,j}^{\mathrm{I}} x_{i,j}^{\mathrm{I}} = 0 \tag{9}$$

where the superscript I denotes the equilibrium compositions at the vapor−liquid interface and $K_{i,j}^{\mathrm{I}}$ represents the vapor−liquid equilibrium ratio for component i on stage j. And the equilibrium constant is computed by

$$K_i^{\mathrm{I}} = \frac{P_i^0 \gamma f_{ii}^0}{P f_i} \tag{10}$$

The Wilson equations for the liquid phase have been selected to calculate the liquid activity coefficient and the equation is expressed in eq 11.

$$\ln\gamma_i = \sum_{j=1}^{c} x_j - \ln\left(\sum_{j=1}^{c} x_j \Lambda_{ij}\right) - \sum_{k=1}^{c} x_k \Lambda_{ki} / \sum_{j=1}^{c} x_j \Lambda_{kj} \tag{11}$$

where $\Lambda_{ij} = (V_j/V_i)\exp(-(\mu_{ij} - \mu_{ii})/R_{\mathrm{g}}T)$ and $\mu_{ij} - \mu_{ii}$ are the binary interaction energy parameters. The data of the binary interaction energy parameters are shown in Table 3. Additionally, the SRK model has been used to compute vapor fugacities, and its equations have not been presented here.

In addition to the above equations, there also have the summation equations for the mole fractions:

$$\sum_{i=1}^{C} x_{i,j} - y_{\mathrm{i,j}} = 0 \tag{12}$$

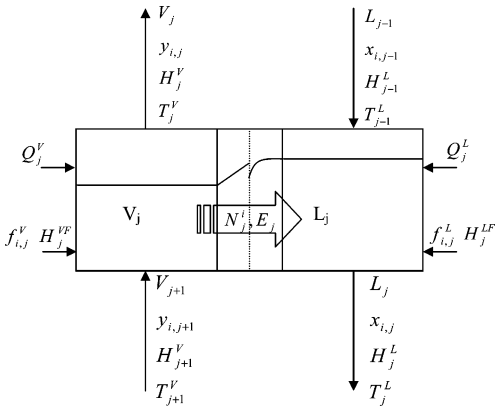

Figure 2. Nonequilibrium stage model.

Table 3. Parameters of Binary Interactive Coefficient

	Parameters of Wilson Model	
component pair	$\mu_{i,j} - \mu_{i,i}$ (J/mol)	$\mu_{j,i} - \mu_{i,i}$ (J/mol)
Me−DMC	788.993069 1	3345.011360
Me−MC	1849.153388	−1410.431382
Me−NH_3	−1305.59000	−1866.88
DMC−MC	−1002.150829	263.4779813
DMC−NH_3	−3891.216926	1678.877164
MC−NH_3	22106.94936	−5825.100416

The vapor pressure equation was given by

$$\log_a P^0 = A + \frac{B}{T + C} + D\ln(T) \tag{13}$$

where P^0 is in kPa and T is in K. The parameters used in the equation are shown in Table 4. For the temperature that excess 405 K, the vapor pressure of ammonia has been extrapolated by the extended Antoine equation.

Thermophysical constants such as density, enthalpy, heat conductivity, viscosity, and surface tension have been calculated based on the correlations suggested by Reid et al.[33] and by Danbert and Danner.[34] Furthermore, the mass-transfer coefficients are computed by the empirical Onda relations.[35]

$$k_{\mathrm{ik}}^L = 0.0051\left(\frac{w^{\mathrm{L}}}{a_{\mathrm{w}} g}\right)^{2/3}\left(\frac{\mu_{\mathrm{m}}^{\mathrm{L}}}{\rho_{\mathrm{m}}^{\mathrm{L}} D_{ik}^{\mathrm{L}}}\right)^{-0.5}\left(\frac{\mu_{\mathrm{m}}^{\mathrm{L}} g}{\rho_{\mathrm{m}}^{\mathrm{L}}}\right)^{1/3}(a_{\mathrm{t}} d_{\mathrm{p}})^{0.4} \tag{14}$$

$$k_{ik}^{\mathrm{V}} = \alpha\left(\frac{w^{\mathrm{V}}}{a_{\mathrm{t}}\mu_{\mathrm{m}}^{\mathrm{V}}}\right)^{0.7}(Sc_{ik}^{\mathrm{V}})^{1/3}(a_{\mathrm{t}} d_{\mathrm{p}})^{-2}\frac{a_{\mathrm{t}} D_{ik}^{\mathrm{V}} p}{p_{\mathrm{Bm}} R_{\mathrm{g}} T} \tag{15}$$

where α is 2.0 for the nonreaction packing of 3.2-mm metal grid ring. The wet area of the packing is estimated using the equations developed by Onda et al.[35] shown as follows:

$$\frac{a_{\mathrm{w}}}{a_{\mathrm{t}}} = 1 - \exp\left[-1.45\left(\frac{w^{\mathrm{L}}}{a_{\mathrm{t}}\mu_{\mathrm{m}}^{\mathrm{L}}}\right)^{0.1}\left(\frac{w^{\mathrm{L}^2} a_{\mathrm{t}}}{\rho_{\mathrm{m}}^{\mathrm{L}^2} g}\right)^{-0.05}\left(\frac{w^{\mathrm{L}^2}}{\rho_{\mathrm{m}}^{\mathrm{L}}\sigma a_{\mathrm{t}}}\right)^{0.2}(\sigma_{\mathrm{C}}/\sigma)^{0.75}\right] \tag{16}$$

The effective interfacial area is estimated using the empirical relation developed by Billet:

$$\frac{a}{a_{\mathrm{t}}} = \frac{1.5}{(a_{\mathrm{t}} 4\epsilon/a_{\mathrm{t}})^{0.5}}\left(\frac{u^{\mathrm{L}} 4\epsilon/a_{\mathrm{t}}}{\mu_{\mathrm{m}}^{\mathrm{L}}/\rho_{\mathrm{m}}^{\mathrm{L}}}\right)^{-0.2}\left(\frac{u^{\mathrm{L}^2}\rho_{\mathrm{m}}^{\mathrm{L}} 4\epsilon/a_t}{\sigma_{\mathrm{m}}^{\mathrm{L}}}\right)^{0.75}\left(\frac{u^{\mathrm{L}^2}}{g 4\epsilon/a_{\mathrm{t}}}\right)^{-0.45} \tag{17}$$

Table 4. Parameters of Vapor Pressure Equation (*P* in kPa and Temperature in K)

	equation parameters					
component	a	A	B	C	D	temperature range (K)
methanol	10.0	7.20587	−1582.271	−33.424	0.0	288.15−357.15
		7.31326	−1669.678	−22.7599	0.0	357.15−613.15
DMC	*e*	51.125	−5991.3	0.0	−5.0971	273.15−548
MC	*e*	6.43419	−2947.93	−116.168	1.14019	250.15−584.15
NH_3	*e*	−3.98661	−1080.33	−74.1328	2.759	180−354.92
		−31.3113	−7.58839	−299.91	6.78079	354.92−405

The mass-transfer coefficients for the reaction zone are estimated using the equations developed by Billet, as follows:

$$k_{ik}^{L}a = 1.13\frac{a_t^{2/3}}{(4\epsilon/a_t)^{0.5}}D_{ik}^{L}0.5\left(\frac{g}{\mu^{L}/\rho^{L}}\right)^{1/6}\mu_m^{L}1/3\frac{a}{a_t} \quad (18)$$

$$k_{ik}^{L}a = 0.275\frac{a_t^{3/2}}{(4\epsilon/a_t)^{0.5}}D_{ik}^{V}\frac{1}{(\epsilon - h_L)^{0.5}}\left(\frac{\mu_m^{V}/\rho_m^{V}}{D_{ik}^{V}}\right)^{1/3}\left(\frac{u_m{}^{V}}{a\mu_m^{V}/\rho_m^{V}}\right)^{3/4}\frac{a}{a_t} \quad (19)$$

Heat-transfer coefficients are predicted using Chilton−Colburn analogy[36,37] as follows

$$h^{V} = k_{av}^{V}C_{pm}^{V}(Le^{V})^{2/3} \quad (20)$$

for vapor phase and

$$h^{L} = k_{av}^{L}C_{pm}^{L}(Le^{L})^{1/2} \quad (21)$$

for liquid phase.

Result and Discussion

The simulated column (see Figure 1), a 2-m-tall stainless steel reactive distillation column with an inner diameter of 22 mm, was configured with two feeding inlets and a side outlet. The materials were fed into the distillation column through a preheater with volumes of 500 mL for each feed stream. It would take about 2−5 h for the feed material to pass through the preheater to the distillation column, which was enough for the complete conversion of urea to MC in the preheater, as the first reaction for DMC synthesis by urea methanolysis method could take place with high yield even in the absence of catalyst. The distillation column was divided into three sections, the rectifying section, the reaction section, and the stripping section. The 100 mL of catalyst pellets weighed 103 g with an average diameter of 3 mm and were randomly packed in the reaction zone, and the grid metal rings with a diameter of 3.2 mm were packed into the nonreaction zones. The distillation configured with a partial condenser to release the noncondensing gas of ammonia and a partial reboiler to discharge the heavy component of MC. The temperature in the reaction zone was set to 454.2 K for the synthesis reaction, and the process was carried out under a pressure of 9−13 atm.

Under the above conditions, the nonequilibrium model was carried out to investigate the performance of the CD process. The CD was distributed for 40 nonequilibrium segments along the distillation column, including the condenser and reboiler. The material mixture of urea and methanol with 20 mol % urea converted to 20 mol % MC, 20 mol % NH_3, and 60 mol % methanol in the preheater and then subsequently fed on stage 14. The flow rate for the materials was 20 mL/h, and pure methanol with a flow rate of 60 mL/h was fed on stage 26. The product was sampled from the side outlet on stage 6 whereas the top liquid flow was totally refluxed to the distillation column.

A Typical Result. Figures 3−8 showed the typical modeling data for the catalytic distillation of the DMC synthesis process from urea and methanol over solid base catalyst, which was operated under the pressure of 9 atm. It should be noticed from Figures 3 and 4 that the concentration of DMC increased in the rectifying zone due to the azeotropic distillation of the binary pair of Me−DMC. The lower concentration of DMC in the liquid phase than that in the vapor phase in the rectifying zone, shown in Figure 5, demonstrated the azeotropic distillation of methanol with the binary azeotropic pair of Me−DMC. Nevertheless, higher DMC composition in the liquid phase than that in vapor phase on stages 17−20 was due to the vaporization of methanol in this area, and then DMC was accumulated to the reaction zone to form the highest values of DMC concentration on stage 19, which were 9.76 and 9.02 wt % for liquid and vapor, respectively. This seemed not suitable for the separation of DMC. Actually, DMC was normally separated from the heavy component of MC and the distillation also showed its superiority on its removal of the noncondenser component of ammonia to restrain the reverse reaction of DMC with ammonia. Furthermore, for the high solubility of ammonia in methanol, the concentration of DMC was decreased near the condenser. As a result, it was reasonable that the products should be sampled from the rectifying zone considering the strong nonideality of this system.

The flow ratio to the total feed for liquid and vapor phases is illustrated in Figure 6. It could be obviously noticed that the liquid and vapor flows continuously decreased from stage 13 to 26, which were due to the effect of column heating on this area. As shown in Figure 6, the considerable decrease in the liquid flow from stage 5 to 6 was caused by the liquid side sample on stage 6, and the methanol feed on stage 26 also caused the decrease in the vapor flow rate from stage 26 to 27. However, the effect of the material feed on stage 14 was not obvious. The reason was due to the effect of column heating, which caused the extreme changes of the liquid and vapor flow rates in the distillation column. Whereas, there was also evidence for the effect of material feeding, such as the composition of DMC on stage 14 being lower than that of each side, as seen from Figure 5. Additionally, it also could be easily observed that the flow ratio to the total feed in the stripping zone was very low because of the effect of heating on the distillation column. This indicated that this area might be deleted for this process and it would be a suggestion for its scale up in industrial application.

The temperature profile along the distillation column is illustrated in Figure 7. It could be seen that the temperature in the condenser was much lower than in the distillation column, which was 94.8 °C, with a large amount of ammonia existing in the condenser. The effect of column heating had raised the temperature from 410.2 to 454.2 K on the stages of 13−26, and the composition of MC consequently increased with the

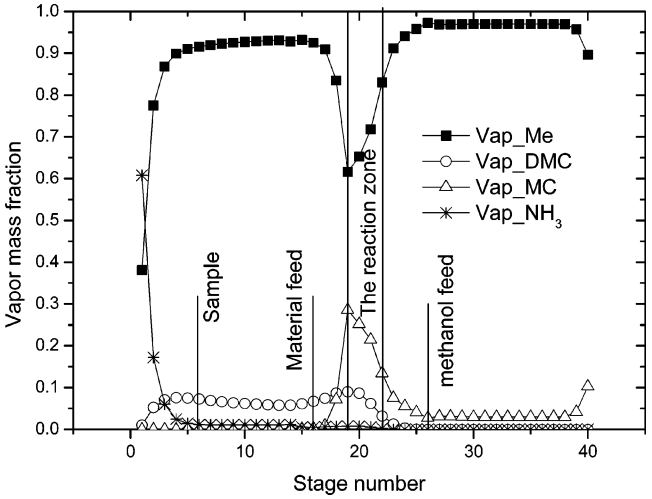

Figure 3. Vapor composition profile along the column.

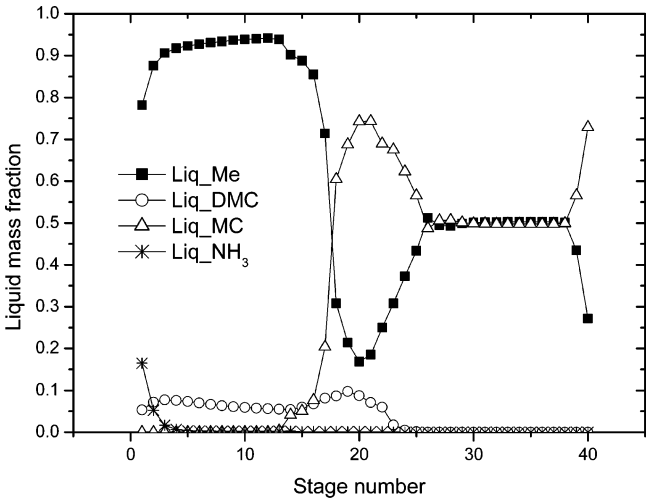

Figure 4. Liquid composition profile along the column.

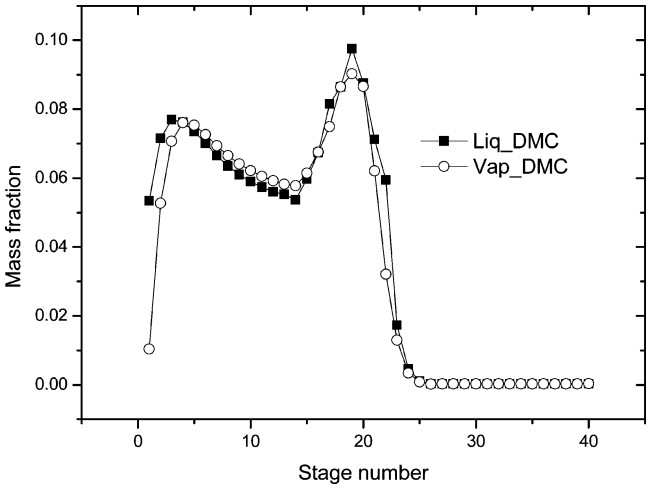

Figure 5. Liquid and vapor concentration of DMC along the column.

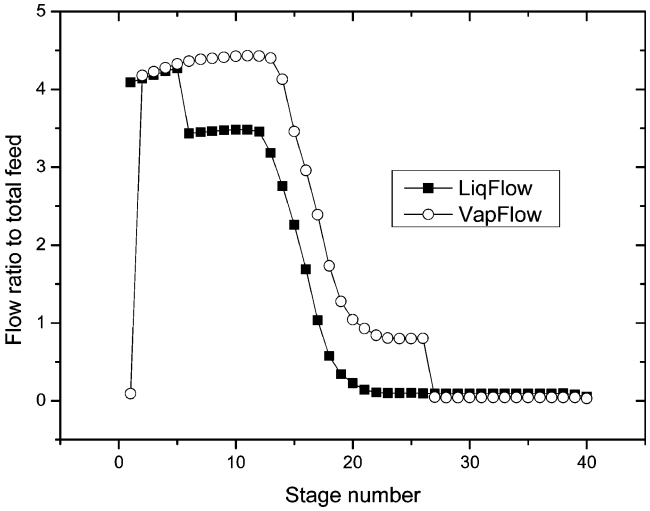

Figure 6. Liquid and vapor flow rate.

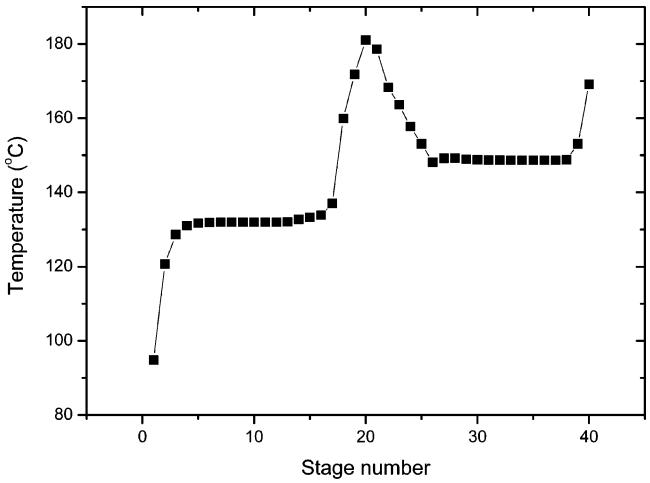

Figure 7. Temperature profile.

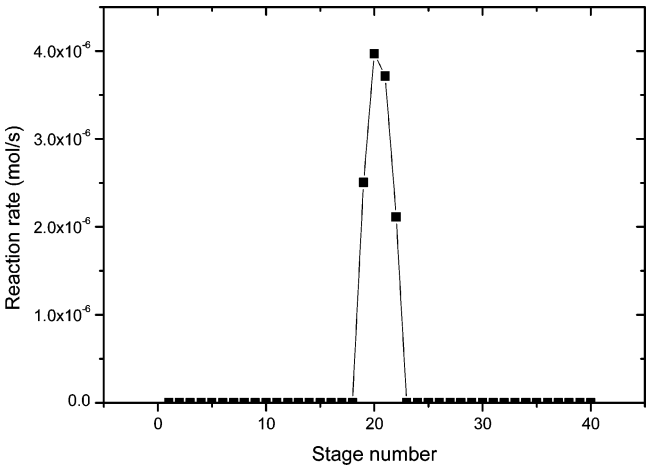

Figure 8. Reaction rate along the column.

vaporization of light components. As a result, the reaction could occur properly in the reaction zone. The temperature in the stripping zone was 421.8 K and the composition of MC in this area was almost constant, whereas the composition of MC increased rapidly when it neared the reboiler.

The reaction rate along the column is demonstrated in Figure 8. The reaction of MC converted to DMC took place on the stages from 19 to 22, which reacted at the temperature of 454.2 K (see Figure 7). The reaction rate reached the maximum value on stage 20 and then continuously decreased along the reaction zone with the consumption of the reactant. The lower reaction rate on stage 19 than that on stage 20 was attributed to the reverse reaction of DMC with NH_3.

Table 5 showed the comparison of the predicted results with the measured data. The estimated results were in qualitative agreement with the experiment data. The compositions of the product flow were 92.7 wt % methanol, 7 wt % DMC, and 0.3

Table 5. Typical Results from Experiment and Predictions for the Synthesis of Dmc

parameter	measured	estimated
temperature of top (°C)	91.0	94.8
temperature of reboiler (°C)	165.3	169.1
T in reaction zone (°C)	180	181.1
material feed (mL/h)	20	20
methanol feed (mL/h)	60	60
yield of DMC (%)	45	45
reflux ratio	4	4
condenser, mass fraction		
Me	0.768	0.782
DMC	0.052	0.053
MC	0	0
ammonia	0.18	0.165
rebloiler, mass fraction		
Me	0.260	0.271
DMC	0	0
MC	0.740	0.729
ammonia	0	0
product, mass fraction		
Me	0.927	0.927
DMC	0.070	0.070
MC	0	0
ammonia	0.003	0.003

wt % ammonia. Consenquently, a further atmospheric distillation and a pressed distillation were needed in order to completely separate the component of DMC. And the materials of methanol and MC could be considered for its proper use as a recycle feed. The temperature of the experiment data was lower than the estimated value in the condenser. This contributed to the fact that the condenser was exposed in the air, which easily was affected by the environment. The lower temperature of the experiment in the reboiler to the predicted result was owed to the unavoidable remaining methanol in the reboiler, which was used for wetting the distillation packages at the start stage of the process.

Effect of Pressure on DMC Yield. As the system included components with a wide range of boiling temperature, the compositions of the components might be greatly affected by the operating pressure in the catalytic distillation process. The data in Figure 9 illustrated the variations of DMC yield with the changes of the operating pressure in the CD process. In this case, the reaction temperature was controlled at the temperature of 454.1 K by a heater on the CD column, which changed within the range of 2 K. It could be seen that DMC yield and the concentration of DMC in the product increased with the raising of the operating pressure. And the concentration of MC in the reaction zone was decreased from 0.82 to 0.61 wt %, where the concentration values were selected on stage 19. This might be appropriate for operation of the DMC synthesis reaction as the increased operating pressure caused the appropriate reactants ratio of Me with MC. This was also proved by the increased composition of DMC in the reaction zone with the operating pressure in Figure 10, which demonstrated the composition profiles of DMC along the CD column under the pressures of 9, 11, and 13 atm, respectively. However, the composition of DMC in the rectifying zone increased relatively slowly as in the reaction zone, owing to the light component of ammonia, which had great solubility in the methanol solvent. Consequently, the increase of pressure was appropriate for the operation of the reaction, while it was disadvantageous to the separation of DMC in the CD process.

Effect of Temperature on DMC Yield. The reaction temperature was an important parameter and could directly increase the reaction rate for the synthesis of DMC. The temperature might be changed by the variation of the operating pressure in a CD process, and it also could be controlled by a

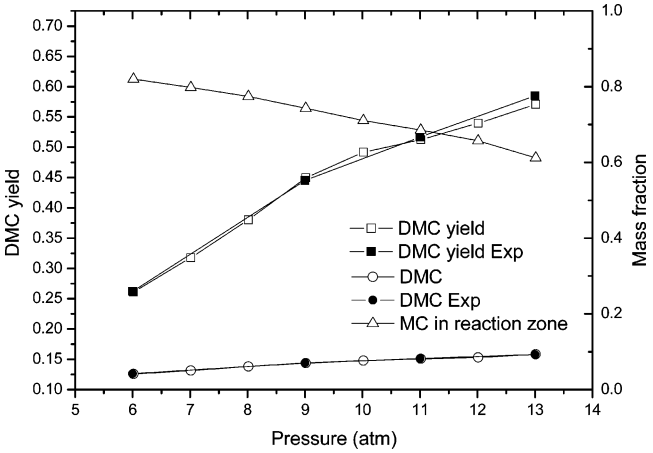

Figure 9. Effect of pressure on DMC yield.

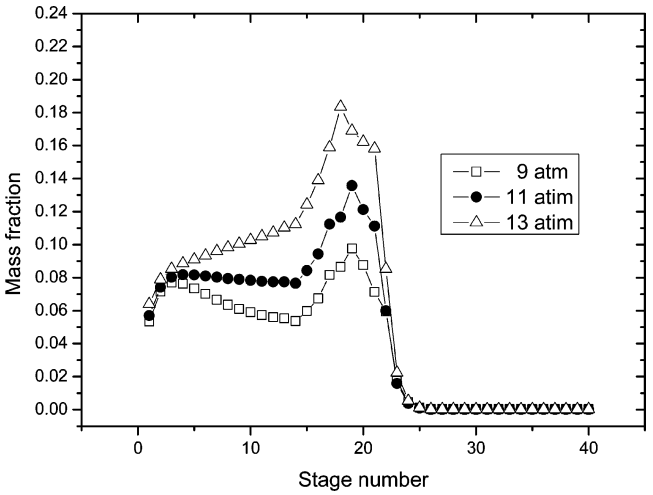

Figure 10. Effect of pressure on DMC composition in the column.

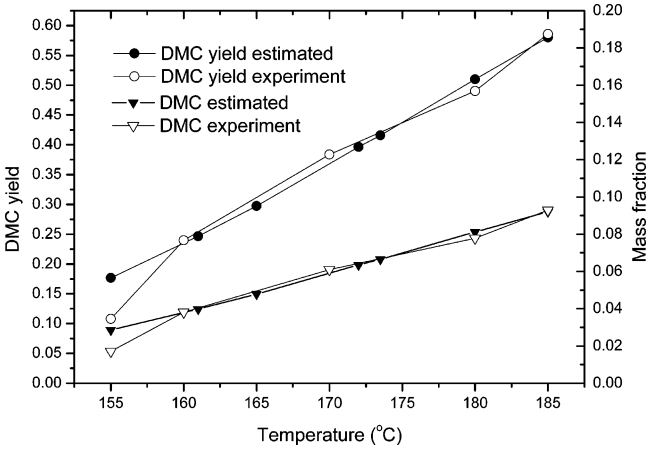

Figure 11. Effect of temperature in the reaction zone on DMC yield.

column heater through changing the compositions of the components in the CD column. The influence of reaction temperature on DMC yield is shown in Figure 11, which comparing the result predicted by the nonequilibrium model with the experimental data operated under a pressure of 10 atm. From Figure 11, it should be noticed that raising the reaction temperature could exactly improve the DMC yield. The reaction temperature on different locations varied due to the interaction of the reaction and the separation in the reaction zone, as shown from Figure 6. So, it was really impossible to keep the temperature constant in the whole reaction zone of the CD column, which might cause the difference between the experi-

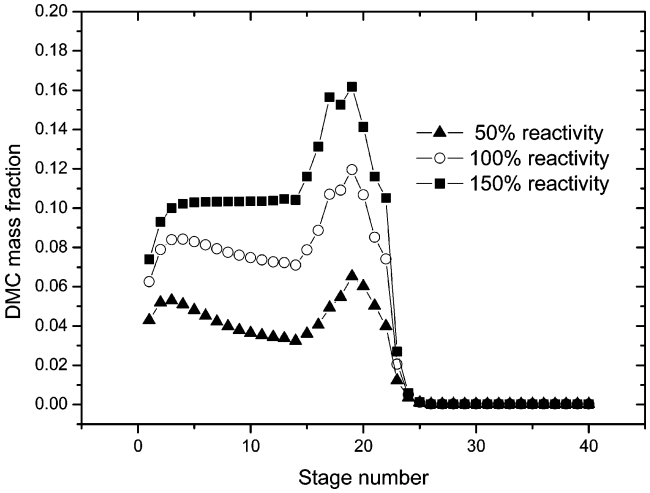

Figure 12. Effect of reaction efficientcy on the DMC.

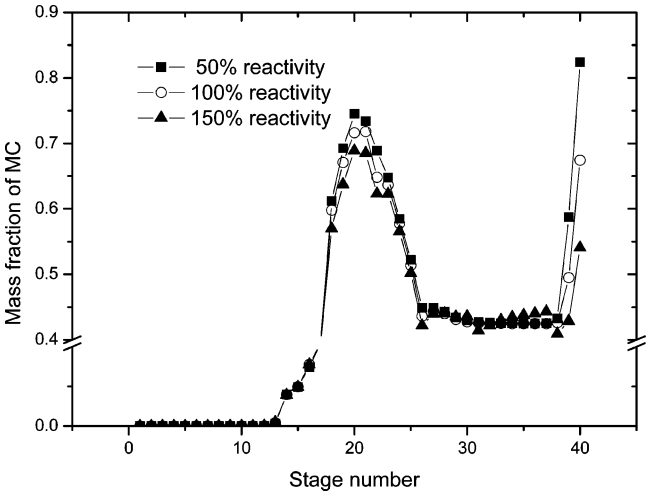

Figure 13. Effect of reaction efficientcy on the MC.

mental data and the predicted result. The predicted result showed qualitatively well with the experimental data except that the experimental data of DMC yield at 428.2 K, which was 10.8%, was much lower than the predicted data of 17.7%.

Effect of Reaction Efficiency. The sensitivity analysis for the process of DMC synthesis from urea and methanol toward the kinetics was carried out by changing ±50% of the reaction rate constant. The computed DMC yields were 28.0 and 64.6%, respectively, whereas the DMC yield for the initial reaction rate constant was 50.1%. The effect of the kinetics on the liquid composition of MC and DMC along the distillation column is illustrated in Figures 12 and 13. It could be observed that the liquid composition of DMC along the distillation column was greatly influenced by the reaction kinetics, whereas the liquid composition of MC along the distillation column was not sensitive to the changes of the kinetics constant. The concentration of MC in the CD column was mainly dependent on the temperature where it was located. Consequently, the CD process of DMC synthesis from urea and methanol over the solid base catalyst was kinetically controlled under the simulated conditions. And the composition of MC was mainly controlled by the column heater.

Conclusions

A nonequilibrium model for the catalytic distillation was developed to investigate the process of the DMC synthesis by the urea methanolysis method over a solid-based catalyst, which was operated in the CD reactor with a diameter of 22 mm at the bench scale. In this case, the Wilson model was used to deal with the nonideality of the liquid phase. Considering the interaction between the chemical reaction and production separation, the superiority of the CD on its removal of the product to restrain the reverse reaction of DMC synthesis was detailed and discussed. And furthermore, the influence of pressure, temperature, and reactive sensitivity was discussed in the present contribution. The pressure influence on DMC yield analysis has shown that the increase of pressure was advantageous for the reaction while it was disadvantageous for product separation. Taking one with the other, the increase of pressure was appropriate for the process of DMC synthesis. Temperature in the reaction zone was an essential parameter for this process as it greatly affected the reaction rate of DMC. The analysis of the sensitivity toward the reaction rate constant indicated that the DMC yield was greatly influenced by the reaction kinetics, and the liquid composition of MC in the distillation was determined by the operation status. The binary azeotrope of DMC and methanol caused DMC rectified from the reaction zone to the rectifying zone in the reactive distillation, whereas it could be destroyed from stage 1 to 3 because of the large solubility of ammonia in the methanol solvent. The inner flow ratio analysis also showed that the stripping zone should be deleted when the process of DMC synthesis was scaled up in industrial production. As the process includes the formation of a binary azeotrope and the removal of the noncondenser component of ammonia, the catalytic distillation was appropriate for the process of DMC synthesis and product separation.

Nomenclature

a = effective interfacial area, m^2 section^{-1}
a = specific interfacial area, m^2 m^{-3}
a_w = wetting specific interfacial area, m^2 m^{-3}
c = total number of components
C_P = heat capacity, J mol^{-1} K^{-1}
C_t = liquid concentration of component, mol L^{-1}
d_P = package diameter, m
D = binary diffusion coefficient, m^2 s^{-1}
e = heat-transfer rate, J s^{-1}
E_a = activity energy for forward reaction, J mol^{-1}
E_{a2} = activity energy for backward reaction, J mol^{-1}
f = gas-phase fugacity coefficient
F = feed flow rate, mol s^{-1}
h = heat-transfer coefficient, J m^{-2} s^{-1} K^{-1}
H = molar enthalpy, J mol^{-1}
Le = Lewis number ($\lambda M \rho^{-1} C_P^{-1} D^{-1}$)
k_1 = forward kinetic rate constant of eq 1, mol L^{-1} s^{-1}
k_2 = backward kinetic rate constant of eq 1, mol L^{-1} s^{-1}
k = binary mass-transfer coefficient mol m^{-2} s^{-1}
K = equilibrium ratio
L = liquid flow rate, mol s^{-1}
N = mass-transfer rate, mol s^{-1}
P = pressure, kPa
P_i^0 = vapor pressure of component i, kPa
Q = heat duty, J s^{-1}
R = reaction rate, mol s^{-1}
R_g = universal gas constant, 8.314 J mol^{-1} K^{-1}
S = sample flow rate, mol s^{-1}
Sc = Schmidt number
T = temperature, K
u = superficial velocity, m s^{-1}
V = vapor flow rate, mol s^{-1}

w = mass flow rate, kg m^{-2} s^{-1}
x = liquid molar fraction
y = vapor molar fraction
z = molar fraction of feed component

Greek letters

γ = liquid phase activity coefficient
ϵ = void fraction, m^3 m^{-3}
η = dimensionless distance
μ viscosity, Pa s
ρ = density, kg m^{-3}
σ = surface tension, N m^{-1}
ω = total amount of catalyst

Subscript

0 = saturated property
av = average value
i = component index
j = section index
k = component index
m = property of mixture

Superscript

I = vapor liquid interface
L = liquid phase
LF = liquid feed
LR = liquid reaction
V = vapor phase
VF = vapor feed

Acknowledgment

Financial support from the National Science Key Foundation (2006BAC02A08) is acknowledged.

Literature Cited

(1) Tundo, P.; Selva, M. The Chemistry of Dimethyl Carbonate. *Acc. Chem. Res.* **2002**, *35*, 706.

(2) Ono, Y. Dimethyl Carbonate for Environmentally Benign Reactions. *Catal. Today* **1997**, *35*, 15.

(3) Pacheco, M. A.; Marshall, C. L. Review of Dimethyl Carbonate (DMC) Manufacture and Its Characteristics as A Fuel Additive. *Energy Fuels* **1997**, *11*, 2.

(4) Rivetti, F. The Role of Dimethyl Carbonate in the Replacement of Hazardous Chemicals. *Stud. Surf. Chem. Catal.* **2000**, *3*, 497.

(5) Wei, T.; Wang, M.; Wei, W.; Sun, Y.; Zhong, B. Synthesis of Dimethyl Carbonate by Transesterification over CaO/Carbon Composites. *Green Chem.* **2003**, *5*, 343.

(6) Romano, U.; Twsel, R.; Maural, M. M.; Rebora, P. Synthesis of Dimethyl Carbonate from Methanol, Carbon Monoxide, and Oxygen Catalyzed by Copper Compounds. *Ind. Eng. Chem. Prod. Res. Dev.* **1980**, *19*, 396.

(7) Itoh, H.; Watanabe, Y.; Moric, K.; Umino, H. Synthesis of Dimethyl Carbonate by Vapor Phase Oxidative Carbonylation of Methanol. *Green Chem.* **2003**, *5*, 558.

(8) Yamamoto, Y.; Matsuzaki, T.; Tanaka, S.; Nishihira, K.; Ohdan, K.; Nakamura, A.; Okamoto, Y. Catalysis and Characterization of Pd/NaY for Dimethyl Carbonate Synthesis from Methyl Nitrite and CO. *J. Chem. Soc., Faraday Trans.* **1997**, *93*, 3721.

(9) Ruixia, J.; Shufang, W.; Xinqiang, Z.; Yanji, W.; Chengfang, Z. The Effects of Promoters on Catalytic Properties and Deactivation Regeneration of the Catalyst in the Synthesis of Dimethyl Carbonate. *Appl. Catal., A* **2003**, *238*, 131.

(10) Wang, M.; Wang, H.; Zhao, N.; Wei, W.; Sun, Y. Synthesis of Dimethyl Carbonate from Urea and Methanol over Solid Base Catalysts. *Catal. Commun.* **2005**, *7*, 6.

(11) Kloker, M.; Kenig, E. Y.; Hoffmann, A.; Kreis, P.; Gorak, A. Rate-based Modelling and Simulation of Reactive Separations in Gas/Vapour-Liquid Systems. *Chem. Eng. Process.* **2005**, *44*, 617.

(12) Agreda, V. H.; Partin, P. H.; Heise, W. H. High Purity Methyl Acetate via Reactive Distillation. *Chem. Eng. Process.* **1990**, *86*, 40.

(13) Pilavachi, P. A.; Schenk, M.; Perez-Cisneros, E.; Gani, R. Modeling and Simulation of Reactive Distillation Operations. *Ind. Eng. Chem. Res.* **1997**, *36*, 3188.

(14) Agar, D. W. Multifunctional Reactors: Old Preconceptions and New Dimensions. *Chem. Eng. Process.* **1999**, *54*, 1299.

(15) Stankiewicz, A. I.; Moulijn, J. A. Process Intensification: Transforming Chemical Engineering. *Chem. Eng. Prog.* **2000**, *96*, 22.

(16) Malone, M. F.; Doherty, M. F. Reactive Distillation. *Ind. Eng. Chem. Res.* **2000**, *39*, 3953.

(17) Tuchlenski, A.; Beckmann, A.; Reusch, D.; DuKssel, R.; Weidlich, U.; Janowsky, R. Reactive Distillation. Industrial Applications, Process Design & Scale-up. *Chem. Eng. Sci.* **2001**, *56*, 387.

(18) Taylor, R.; Krishna, R. *Multicomponent Mass Transfer*; John Wiley and Sons: New York, 1993.

(19) Podrebarac, G. G.; Ng, F. T. T.; Rempel, G. L. The Production of Diacetone Alcohol with Catalytic Distillation. II. A Rate-based Catalytic Distillation Model for the Reaction Zone. *Chem. Eng. Sci.* **1998**, *53*, 1077.

(20) Higler, P.; Taylor, R.; Krishna, R. Nonequilibrium Modelling of Reactive Distillation: Multiple Steady States in MTBE Synthesis. *Chem. Eng. Sci.* **1999**, *54*, 1389.

(21) Kenig, E.; Jakobsson, K.; Banik, P.; Aittamaa, J.; Górak, A.; Koskinen, M.; Wettmann, P. An Integrated Tool for Synthesis and Design of Reactive Distillation. *Chem. Eng. Sci.* **1999**, *54*, 1347.

(22) Sundmacher, K.; Hoffmann, U. Development of A New Catalytic Distillation Process for Fuel Ethers via A Detailed Nonequilibrium Model. *Chem. Eng. Sci.* **1996**, *51*, 2359.

(23) Lee, J. H.; Dudukovic, M. P. A Comparison of the Equilibrium and Nonequilibrium Models for A Multicomponent Reactive Distillation Column. *Comput. Chem. Eng.* **1998**, *23*, 159.

(24) Taylor, R.; Krishna, R. Modelling Reactive Distillation. *Chem. Eng. Sci.* **2000**, *55*, 5183.

(25) Higler, A. P.; Taylor, R.; Krishna, R. Nonequilibrium Modeling of Reactive Distillation: A Dusty Fluid Model for Heterogeneously Catalyzed Processes. *Ind. Eng. Chem. Res.* **2000**, *39*, 1596.

(26) Zheng, Y.; Ng, F. T. T.; Rempel, G. L. Process Analysis for the Production of Diacetone Alcohol via Catalytic Distillation. *Ind. Eng. Chem. Res.* **2003**, *42*, 3962.

(27) Huss, R. S.; Chen, F.; Malone, M. F.; Doherty, M. F. Reactive Distillation for Methyl Acetate Production. *Comput. Chem. Eng.* **2003**, *27*, 1855.

(28) Bravo, J. L.; Pyhalathi, A.; Jaervelin, H. Investigations in a Catalytic Distillation Pilot Plant: Vapor/Liquid Equilibrium, Kinetics and Mass Transfer Issues. *Ind. Eng. Chem. Res.* **1993**, *32*, 2220.

(29) Sneesby, M. G.; Tade, M. O.; Smith, T. N. Steady State Transitions in the Reactive Distillation of MTBE. *Comput. Chem. Eng.* **1998**, *22*, 879.

(30) Sundmacher, K.; Uhde, G.; Hoffmann, U. Multiple Reactions in Catalytic Distillation Processes for the Production of the Fuel Oxygenates MTBE and TAME: Analysis by Rigorous Model and Experimental Validation. *Chem. Eng. Sci.* **1999**, *54*, 2839.

(31) Luo, H. P.; Xiao, W. D. A Reactive Distillation Process for A Cascade and Azeotropic Reaction System: Carbonylation of Ethanol with Dimethyl Carbonate. *Chem. Eng. Sci.* **2001**, *56*, 403.

(32) Wang, M. H.; Zhao, N.; Wei, W.; Sun, Y. H. Synthesis of Dimethyl Carbonate from Urea and Methanol over ZnO. *Ind. Eng. Chem. Res.* **2005**, *44*, 7596.

(33) Reid, R. C.; Prausnitz, J. M.; Poling, B. E. *The Properties of Gases and Liquids*; McGraw-Hill Professional: New York, 1987.

(34) Danbert, T. E.; Danner, R. P. *Physical and Thermodynamics Properties of Pure Chemicals: Data Compilation*; Hemisphere Publishing Corp.: New York, 1989.

(35) Onda, K.; Takeuchi, H.; Okumoto, Y. Mass Transfer Coefficients between Gas and Liquid Phase in Packed Columns. *J. Chem. Eng. Jpn.* **1968**, *1*, 56.

(36) King, C. J. *Separation Process*; McGraw-Hill Professional: New York, 1980.

(37) Xu, Y.; Zheng, Y.; Ng, F. T. T.; Rempel, G. L. A Three-phase Nonequilibrium Dynamic Model for Catalytic Distillation. *Chem. Eng. Sci.* **2005**, *60*, 5637.

Received for review November 21, 2006
Revised manuscript received September 10, 2007
Accepted September 11, 2007

IE061480R